5. Usher A et al. *Phys. Rev. B* **41** 1129 (1990)
6. Maude D K et al. *Phys. Rev. Lett.* **77** 4604 (1996)
7. Aifer E H, Goldberg B B, Broido D A *Phys. Rev. Lett.* **76** 680 (1996)
8. Schmeller A et al. *Phys. Rev. Lett.* **75** 4290 (1995)
9. Barrett S E et al. *Phys. Rev. Lett.* **74** 5112 (1995)
10. Belavin A A, Polyakov A M *Pis'ma Zh. Eksp. Teor. Fiz.* **22** 245 (1975) [*JETP Lett.* **22** 245 (1975)]
11. Sondhi S L et al. *Phys. Rev. B* **47** 16419 (1993)
12. Fertig H A et al. *Phys. Rev. B* **50** 11018 (1994)
13. Apel W, Bychkov Yu A *Phys. Rev. Lett.* **78** 2188 (1997)
14. Bychkov Yu A, Maniv T, Vagner I D *Phys. Rev. B* **53** 10148 (1996)
15. Wilczek F, Zee A *Phys. Rev. Lett.* **51** 2250 (1983)
16. Rajaraman R *Solitons and Instantons: an Introduction to Solitons an Instantons in Quantum Field Theory* (Amsterdam: North-Holland, 1982)

Nonlinear screening, and spin and cyclotron gaps in the 2D electron gas of GaAs/AlGaAs heterojunctions

V T Dolgopolov, A A Shashkin, A V Aristov, D Schmerek, W Hansen, J P Kotthaus, M Holland

We use AlGaAs/GaAs single-heterojunction samples that contain, apart from a metallic gate on the front surface, a highly doped (4×10^{18} cm^{-3} Si) layer of thickness 200 A in the bulk of the GaAs. This layer remains well-conducting even at very low temperatures and serves as a back electrode. Whereas in standard AlGaAs/GaAs heterostructures the electrons of a 2DEG originate from a doped layer in the AlGaAs barrier, the 2DEG in our samples is created in a similar way to Si MOSFET's: the 2DEG is field-effect-induced at a positive bias V_g applied to the front gate with respect to the back contact. The bottom of the conduction band in our structure is shown in the inset to Fig. 1. A blocking barrier between the gate and the 2DEG is formed by a short-period GaAs/AlAs superlattice capped by a thin GaAs layer. A wide but shallow tunnel barrier between the back electrode and the 2DEG is created by the weak residual p-doping of the GaAs layer. The electron transfer across this tunnel barrier establishes an equilibrium between the back contact and the 2DEG.

By modulating V_g with a small ac voltage, we measure the ac current through the sample. The real part of the current depends on the tunnel resistance [1, 2] while the imaginary component is determined by the capacitance of the structure. Unlike in earlier magneto-capacitance measurements, we avoid spurious lateral transport effects using the back electrode parallel to the 2DEG. From this back electrode the electron system is charged through a tunnel barrier, regardless of the value of σ_{xx} in the 2DEG.

In our experiments [3] we studied the imaginary component of the ac current through the sample as a function of the gate voltage ($C-V$ curves). We worked in the frequency range 100 Hz to 10 kHz at magnetic fields of up to 16 T and a temperature of 25 mK. The amplitude of the ac voltage did not exceed 1 mV and corresponded to the linear regime. The majority of the measurements presented here were performed on three samples. The gate areas were 9200 μm^2 for one, and 870 μm^2 for the others.

Typical experimental dependences of the low-frequency sample capacitance upon gate voltage are presented in Fig. 2. The data were recorded at temperature ≈ 25 mK, but we checked that below 1 K all the $C(V)$ curves were temperature independent. Already for small magnetic fields the data clearly show the typical filling factor dependence of the capacitance signal: the capacitance signal oscillates with minima at integer filling factors, and an enhanced capacitance with respect to the zero field value occurs between the minima. This behaviour reflects the strong modulation of the thermodynamic density of states (DOS) by the magnetic field.

In order to convert the low-frequency $C-V$ curve $C_{low}(V_g)$ into the dependence of DOS on the gate voltage, we use the following procedure: (i) We find the high-frequency limit of the sample capacitance $C_{high}(V_g)$ (see Fig. 2). (ii) The distance x_w as a function of gate voltage is determined from the $C-V$ curve at $B = 1$ T using relation [1]

$$\frac{2eB}{h} = \frac{\kappa}{ex_w} \int_{\Delta V_{LL}} \frac{C_{low} - C_{high}}{C_{high}} \, dV_g . \qquad (1)$$

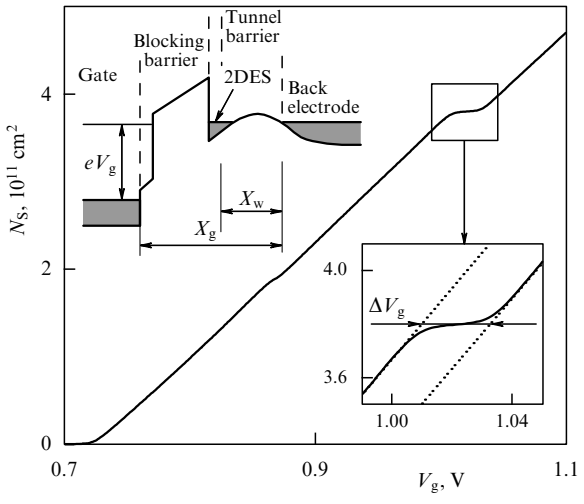

Figure 1. Electron density in the 2DES as a function of the gate voltage in a magnetic field $B = 8$ T. A blow-up of the $\nu = 2$ plateau region shows the way to determine the plateau width. A sketch of the band diagram of the device is displayed in the inset.

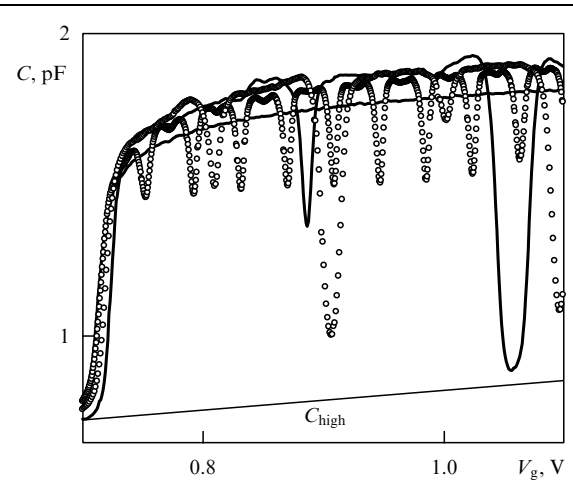

Figure 2. Experimental gate voltage dependences of the structure capacitance on the small area sample in different magnetic fields: $B = 0$ (solid line), 1 T (open circles), 5 T (dots), 9 T (bold line). The value used for $C_{high}(V_g)$ is also shown.

The dependence $x_g(V_g)$ is obtained from the $C-V$ curve in the absence of a magnetic field. (iii) Finally, using the equation

$$\frac{C_{low}-C_{high}}{C_{high}}=\frac{e^2D^*x_w^2}{e^2D^*x_w(x_g-x_w)+\kappa x_g}\,, \tag{2}$$

we recover the dependence $D^*(V_g)$.

From the experimental curves in Fig. 2 we also obtain the electron density N_s in the 2DEG as a function of V_g (see Fig. 1):

$$dN_s = dV_g\,\frac{x_g}{x_w}\,\frac{C_{low}-C_{high}}{Ae}\,, \tag{3}$$

where A is the sample area. Thus, we obtain from experimental data both the gate voltage dependent electron density $N_s(V_g)$ and the thermodynamic density of states $D^*(V_g)$ for each value of the magnetic field B.

We have converted these data into the DOS as a function of the Fermi energy $D^*(E_F)$ and into a dependence of the level width Γ on Fermi energy (Fig. 3).

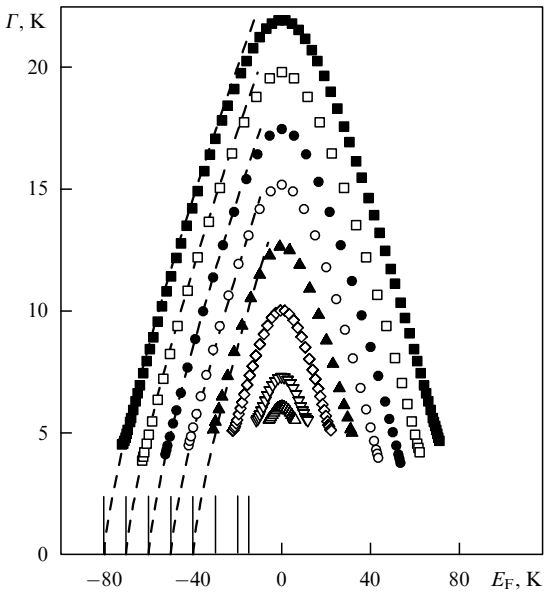

Figure 3. Level width Γ as a function of the Fermi energy at $\nu \approx 2$ for the following values of magnetic field: 1.5 T (△), 2 T (▽), 3 T (◇), 4 T (▲), 5 T (○), 6 T (●), 7 T (□), 8 T (■). Vertical lines mark positions of the lower LL centre $E_F = -\hbar\omega_c/2$. Dashed lines represent a fit by Eqn (4) with $\alpha = 0.82$ and $\gamma = 0.79$.

The dependences $\Gamma(E_F)$ turn out to be very similar for different magnetic fields: the part of the curve corresponding to a lower field B_1 can be obtained by shifting the curve for a higher field B_2 by an energy $[\hbar\omega_c(B_2)-\hbar\omega_c(B_1)]/2$ (see the dashed lines in Fig. 3). This means that over a wide range of magnetic fields the level width Γ has exactly the same dependence upon the Fermi energy counted from the Landau level centre (the values of Γ are found to be large compared to the expected spin splitting at $\nu \approx 2$). We find that on a double logarithmic scale, part of the curve $\Gamma(E_F < 0)$, as a function of $E_F + \hbar\omega_c/2$, is well approximated by a straight line. Taking into account the symmetry of the Γ traces, we conclude that over a wide energy range (except for the vicinity of $E_F = 0$) the level width shows a power-law dependence

$$\Gamma(E_F) = \alpha\left|E_F \pm \frac{\hbar\omega_c}{2}\right|^{\gamma} \tag{4}$$

with exponent $\gamma = 0.79$. It is interesting to note that in a slightly narrower energy interval the reciprocal of the thermodynamic DOS can also be described by a power-law dependence

$$\frac{1}{D^*(E_F)} \propto \left|E_F \pm \frac{\hbar\omega_c}{2}\right|^{\gamma_D} \tag{5}$$

with exponent $\gamma_D = 1.86$ which is approximately twice as large as γ. Moreover, we find that the relation

$$\left[D^*(E_F)\right]^{-1} \propto \Gamma^2(E_F) \tag{6}$$

is valid with good accuracy for all E_F studied, except energies close to the Landau level centre. In particular, this remains true near the midpoint between the Landau levels where both of the Landau levels contribute equally to the DOS value.

It is interesting that the exponent obtained $\gamma \approx 0.8$ is not very different from the widely used value of 0.5 corresponding to $\Gamma \propto B^{1/2}$. Nevertheless this difference results in a drastic change in the behaviour of D^* from exponential to power-law behaviour.

Screening effects in strong magnetic fields have been considered from the theoretical point of view in a number of publications [4–6, 8]. In fact, one can distinguish between two theoretical approaches: (i) calculations of $\Gamma(E_F)$ and $D^*(E_F)$ in the self-consistent Born approximation allowing for screening [4–6]; (ii) a qualitative model of 'threshold screening' [7]. The latter model presumes that for the long-range screened potential the Fermi level lies at the very edge of the fluctuations of a Landau level, i.e.

$$\Gamma(E_F) \approx \left|E_F \pm \frac{\hbar\omega_c}{2}\right|. \tag{7}$$

Here E_F is again counted from the midgap and only the nearest Landau level is considered. In the case of a uniform distribution of charge centres in the space surrounding the 2DEG, for the thermodynamic DOS [7] this theory yields

$$D^*(E_F) \approx \frac{e^2N}{4\pi\kappa\Gamma^2(E_F)}\,, \tag{8}$$

where N is the bulk concentration of charged impurities. This relation is in excellent agreement with our experimental findings (6). From the experimental data using Eqn (8) we find a sensible value of $N \approx 10^{14}$ cm^{-3}.

It is easy to show that the self-consistent Born approximation, as used in several numerical studies [4–6], contains Eqn (8) in an implicit form.

The experimental method employed here to determine the spin gap is based on the measurement of the electron density N_s of a 2DES in a quantized magnetic field as a function of the gate voltage [9]. In Figure 1, we depict the corresponding data that were determined from our capacitance measurements. At gate voltages of $V_g = 0.87$ V and $V_g = 1.02$ V, plateau-like structures are discernible that reflect the reduced density of states in the spin and cyclotron gaps, respectively: when the Fermi level μ lies in a gap of the energy spectrum, the 2DES

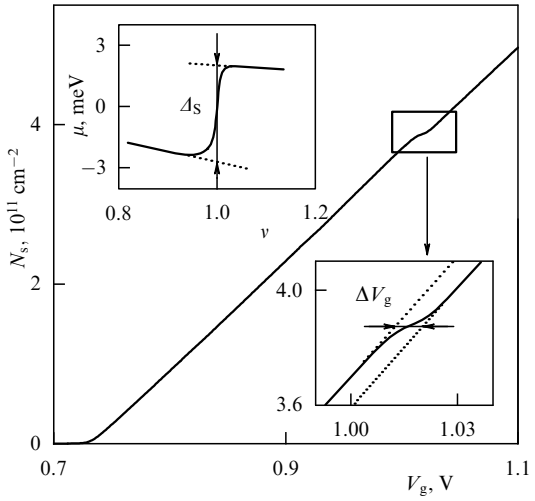

Figure 4. Dependence of the electron density on gate voltage at $B = 16$ T. The plateau region for $\nu = 1$ is blown up. The inset shows the corresponding chemical potential jump calculated from the thermodynamic density of states.

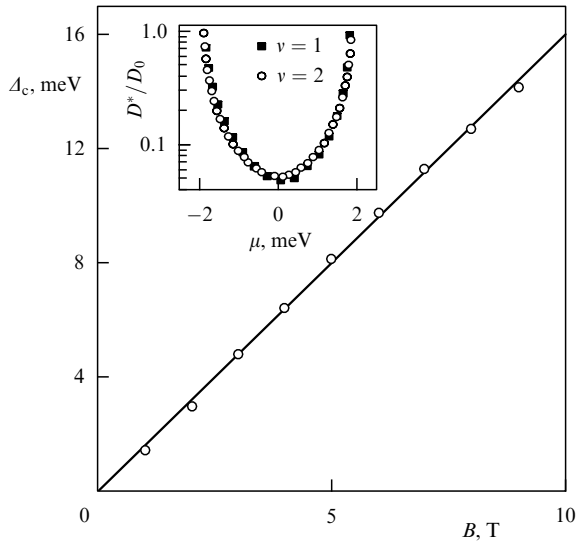

Figure 5. Change of the cyclotron gap at $\nu = 2$ with a magnetic field. The behaviours of the thermodynamic density of states in the spin gap at $B = 16$ T and cyclotron gap at $B = 3$ T are compared in the inset.

does not screen an incremental electric field so that a plateau arises in the dependence $N_s(V_g)$. The plateau width is obtained by linear extrapolation of the density dependence as shown in the second inset of Figs 1 and 4. If the density of states in the centre of the Landau levels is sufficiently high, the extrapolated straight lines reflect the geometrical capacitance given by the distance between the front gate and the 2DES to a good approximation. If the back contact and the 2DES remain in equilibrium, the plateau width directly reflects the jump of the chemical potential between the centres of adjacent Landau levels:

$$\Delta V_g = \frac{x_g}{x_w}\,\frac{\Delta\mu}{e}\,. \tag{9}$$

In Figure 5 the chemical potential jump for the cyclotron gap at $\nu = 2$ is depicted as a function of the magnetic field. This linear dependence corresponds, taking account of the Zeeman splitting, to an effective mass of $0.071m_0$ (m_0 is the free electron mass) which is close to the value of $0.070m_0$ found in cyclotron resonance studies on similar samples [10]. Assuming that the deviation of the data from the straight line in Fig. 5 is due to experimental uncertainty, we can evaluate the accuracy with which we determine the spin gap with the same procedure (Fig. 4). In the range of chemical potential jumps from 1.7 to 14 meV our procedure provides better than 10% accuracy in determining gaps in the spectrum.

Figure 6 shows the behaviour of the spin gap with changing magnetic field. The range of magnetic fields used is chosen so that the spin gap values fall within the above indicated energy interval. To our surprise, the data are best described by a proportional increase of the spin gap with magnetic field.

In Figure 6 we compare the data derived with the help of the procedure described above with the results of two alternative methods for the determination of the chemical potential jump at a filling factor $\nu = 1$. In the first method, that, for example, was applied in Ref. [11], we extract from the experimental data the dependence of the thermodynamic density of states on the electron density [3] and then calculate the chemical potential as a function of the filling factor. The

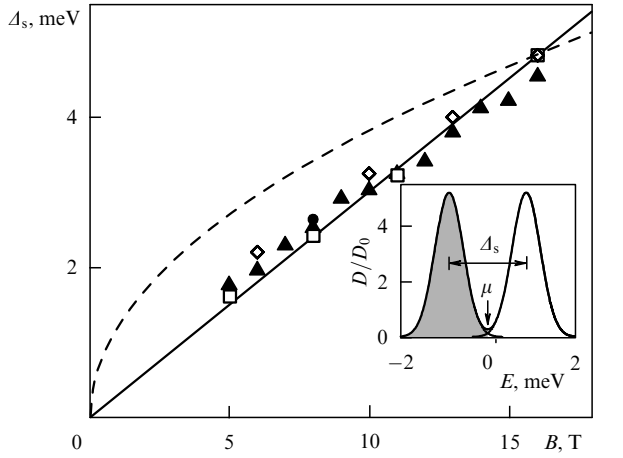

Figure 6. Behaviour of the spin gap at $\nu = 1$ with changing magnetic field. The values of the spin gap are obtained from the plateau width (triangles), the conversion of the thermodynamic density of states (diamonds) and the comparison of the thermodynamic densities of states in the cyclotron and spin gaps (squares). The spin gap value (dot) taken from optical studies [13] is also shown. The solid line corresponds to the effective Landé factor $g \approx 5.2$. The dashed line is a square-root dependence drawn for comparison through the maximum-field point, which is expected from a simple theory, ignoring a numerical factor. The inset displays the profile of the density of states for the spin sublevels at $\nu = 1$ in a magnetic field of 5 T.

corresponding result for $B = 16$ T is displayed in the inset to Fig. 4. The linear extrapolation of the dependence $\mu(\nu)$ at $\nu < 1$ and $\nu > 1$ as shown in the inset of Fig. 4 defines the jump of the chemical potential. We note that this method is less accurate. Firstly, it requires extrapolation over a larger interval of filling factors. Secondly, the jump $\Delta\mu$ is much more sensitive to the value of x_g and, thirdly, the actual extrapolation law is unknown†. In the second method we use

† To solve a similar problem with the chemical potential jump at fractional filling factors an additional fitting parameter (the width of the Gaussian density distribution) was introduced in Ref. [11].

an empirical procedure to determine the spin gap. Here the thermodynamic density of states $D^*(\mu)$ at $\nu \approx 1$ is compared to that at $\nu \approx 2$ in different magnetic fields. If the fields are chosen so that the gaps are equal, the dependences $D^*(\mu)$ can be expected to coincide. An example is given in the inset of Fig. 5. As can be seen from Fig. 6, the data points obtained with the help of all three methods are close to a straight line corresponding to a constant Landé factor $g \approx 5.2$. Within experimental uncertainty this behaviour cannot be described by a square-root dependence as indicated by the dashed line in Fig. 6.

The observed linear dependence of the spin gap on the magnetic field is very similar to that found in activation energy studies [12]. According to Ref. [12], the activation energy for $\nu = 1$ changes approximately linearly with magnetic field over the range 1.2 to 8 T. The corresponding g factor is about 7, which is appreciably larger than the value observed here. The difference is likely to be due to particularities of the activation energy method because at $\nu = 2$ the measured gap also exceeds the cyclotron splitting $\hbar\omega_c$ by 40%. Since, in theory, the gap values obtained by the activation technique may, because of disorder, only be smaller than gaps in the spectrum, the actual origin of the discrepancy remains to be seen. We note that optical investigations yield values of the spin gap at a filling factor $\nu = 1$ and of the cyclotron gap at $\nu = 2, 4$ [13], which are consistent with our data.

A simple estimate of the Coulomb exchange energy $e^2/\kappa l$ (where l is the magnetic length) gives values that are about an order of magnitude larger than the experimentally determined spin gaps. Two physical mechanisms may lead to decreasing exchange energy: the nonzero thickness of the 2DES and the disorder broadening of quantum levels. With the 2DES thickness and the level width as adjustable parameters, Smith et al. [14] succeed in describing the magnetic field dependence of the spin gap found in Ref. [12]. In our case, knowing the density of states we easily found the width and overlap of quantum levels [3]. The behaviour of the density of states $D(E)$ at $\nu = 1$ for the lowest magnetic field used is shown in the inset to Fig. 6. One can see that the corrections to the exchange energy due to level overlap do not exceed 1% at $B \geqslant 5$ T. As far as the finite thickness of the 2DES is concerned, it gives rise to a considerable decrease in the exchange energy at high magnetic fields while in the low-field limit its effect is negligible. Hence, this mechanism alone fails to provide an increase of the power of the theoretical square-root dependence $\Delta_s(B)$. Obviously, the approach [14] does not explain our experimental data at strong magnetic fields.

According to a recent model [15, 16], skyrmion-caused modification of the excitation spectrum at odd integer fillings results in a stronger change of Δ_s with magnetic field in the region of competition between the Zeeman and Coulomb energies. Measurements of the activation energy in tilted magnetic fields [17] indicate that the change of the spin gap attributed to skyrmion effects is smaller than 10% if $g\mu_B B/(e^2/\kappa l) \geqslant 0.015$. Using this condition we estimate that in our experiment the skyrmion effects can be neglected at $B \geqslant 5$ T. In our opinion, the theory's failure to explain the obtained experimental data is caused by the fact that the many-particle phenomena should be very sensitive to correlations of a disorder potential which is present in real systems. Thus, more theoretical work is needed taking into account disorder effects.

This work was supported in part by Volkswagen-Stiftung under Grant No. I/71162 , by the Programme "Nanostructures" from the Russian Ministry of Sciences and by the Russian Foundation for Basic Research under Grant No. 97-02-16829.

References

1. Ashoori R C, Silsbee R H *Solid State Commun.* **81** 821 (1992); Ashoori R C, Ph D Thesis (New York: Cornell University, 1992)
2. Dolgopolov V T et al. *Phys. Rev. B* **51** 7958 (1995)
3. Dolgopolov V T et al. *Phys. Low-Dim. Struct.* **6** 1 (1996)
4. Ando T, Murayama Y *J. Phys. Soc. Jpn.* **54** 1519 (1985)
5. Cai W, Ting C S *Phys. Rev. B* **33** 3967 (1986)
6. Xie X C, Li Q P, Das Sarma S *Phys. Rev. B* **42** 7132 (1990)
7. Shklovskiĭ B I, Éfros A L *Pis'ma Zh. Eksp. Teor. Fiz.* **44** 520 (1986) [*JETP Lett.* **44** 669 (1986)]
8. Kukushkin I V, Meshkov S V, Timofeev V B *Usp. Fiz. Nauk* **155** 219 (1988) [*Sov. Phys. Usp.* **31** 511 (1988)]
9. Dolgopolov V T et al. *Phys. Rev. Lett.* **79** 729 (1997)
10. Drexler H et al. *Semicond. Sci. Technol.* **7** 1008 (1992)
11. Eisenstein J P, Pfeiffer L N, West K W *Phys. Rev. B* **50** 1760 (1994)
12. Usher A et al. *Phys. Rev. B* **41** 1129 (1990)
13. Kukushkin I V, Timofeev V B *Adv. Phys.* **45** 147 (1996)
14. Smith A P, MacDonald A H, Gumbs G *Phys. Rev. B* **45** 8829 (1992)
15. Sondhi S L et al. *Phys. Rev. B* **47** 16419 (1993)
16. Fertig H A et al. *Phys. Rev. B* **50** 11018 (1994)
17. Schmeller A et al. *Phys. Rev. Lett.* **75** 4290 (1995)

Effective action and Green's function for a compressible QH edge state

L S Levitov, A V Shytov, B I Halperin

The edge of a quantum Hall (QH) system plays a central role in charge transport, because the edge states carry Hall current [1]. Also, for odd-denominator Landau level filling factors ν that correspond to incompressible quantized Hall states, the excitations on the edge form a strongly interacting one-dimensional system, which has drawn a lot of interest [2, 3]. The theoretical picture of the QH edge is based on chiral Luttinger liquid (χLL) models, involving either one or several chiral modes which may travel in the same or in opposite directions.

Another important part of the QH theory is the fermion-Chern–Simons approach, which can describe compressible QH states at even-denominator fractions such as $\nu = 1/2$, as well as the incompressible states [4, 5]. In this approach, the fractional QH effect is mapped onto the integer QH problem for new quasiparticles, composite fermions [6], which interact with a statistical Chern–Simons gauge field such that each fermion carries with it an even number p of quanta of the Chern-Simons magnetic flux. The structure of the edge can then be obtained from Landau levels for composite fermions in the average residual magnetic field [7].

Below we present a theory [12] of tunneling into the QH edge based on the composite–fermion picture. We find that under certain conditions the $I-V$ curve is described by a power-law $I \propto V^\alpha$. The tunneling exponent α depends only on the conductivity and interaction in the bulk, and is insensitive to the detailed structure of the edge. In this case the main effect results from the relaxation of electromagnetic disturbance caused by a tunneling electron, in which we include charge and current densities as well as the Chern–Simons